Available online at www.sciencedirect.com

ScienceDirect

Procedia CIRP 74 (2018) 425–429

www.elsevier.com/locate/procedia

10th CIRP Conference on Photonic Technologies [LANE 2018]

Weakening of thick steel plates by laser radiation for the removal of hazardous substances

Christian Hoff[a,]*, Jörg Hermsdorf[a], Stefan Kaierle[a], Ludger Overmeyer[a]

[a]*Laser Zentrum Hannover e.V., Hollerithallee 8, 30419 Hannover, Germany*

* Corresponding author. Tel.: +49-511-2788-237; fax: +49-511-2788-100. *E-mail address:* c.hoff@lzh.de

Abstract

Hazardous substances such as unexploded ordnance represent a serious threat. It is necessary to develop new methods and equipment for their elimination. For this reason, a laser ablation process is developed where the shell of the objects are weakened in a defined manner to reduce the threat to the environment. This article shows how 25 mm thick steel sheets can be weakened with ablation rates of more than 3000 mm³/min and achieved ablation depths of more than 15 mm by means of an adapted process strategy and an off-axis process gas control. Despite the high incoming process energy, it is ensured that there is no danger to affect the hazardous substances. A critical temperature of 300 °C is not exceeded at the rear surface of the sheet metal.

Peer-review under responsibility of the Bayerisches Laserzentrum GmbH.

Keywords: laser ablation; thick metal processing; high speed ablation; macro metal weakening

1. Introduction

Laser ablation in the macro range is recommended as soon as hard materials, short process times, large aspect ratios and high demands on precision and process controllability are required. The case of unexploded ordnance (UXO) considered here represents a serious threat to the society in many parts of the world today and in the future. In Germany alone, an average of 2000 tonnes of UXO are still being discovered each year [1]. Defusing and controlled demolitions are related to large limitations in public life, enormous costs, particularly in urban areas and there is an even exorbitantly higher threat to the explosive ordnance disposal (E.O.D.). Therefore it is urgently necessary to provide the E.O.D. with the most suitable methods and devices to reduce the danger.

This paper presents results from such a laser technology based process development. Due to technical purposes, the use of currently available defusing systems is often not possible. In many cases, only the controlled demolition of the weapon remains as a last choice, leading to large explosive damage and costly evacuations. The process development aims for preventing this explosive damage. Through the laser ablation process, a longitudinal groove is introduced into the steel shell of the objects, where the level of weakening is defined. This causes a substantial reduction of the possible pressure and thus a reduction of the resulting detonation force. By this laser-induced weakening of the ordnance shell and a subsequently controlled, low energy input, a deflagration should be triggered. The resulting pressure will rupture the shell and the detonator will be ejected (see Figure 1). The objective is the development of a sufficiently fast process. In addition, safety must be ensured so that no unintentional ignition of the hazardous substance is initiated. For this purpose, the critical temperature must not exceed 300 °C (specification of E.O.D. / Flash Point TNT 240 °C [2]), on the underneath of the steel sheet. This is critical as it is many times lower than the melting temperature of steel (1150-1500 °C depending on the carbon content [3]).

Peer-review under responsibility of the Bayerisches Laserzentrum GmbH.
10.1016/j.procir.2018.08.166

Fig. 1 UXO defused by low order detonation

1.1. State of the Art

The laser ablation can be divided into three principles: sublimation ablation, melt/flame ablation and oxide chipping. Currently, only low average laser powers are available resulting in relatively achievable ablation rates for sublimation ablation and oxide chipping. Siegel et.al. determine a maximum ablation rate of only ~8 mm³/h for iron [4]. In contrast to this, ablation rates of more than 1500 mm³/min can be achieved with the flame ablation [5]. For the defined ablation of wall thicknesses up to 25 mm, the focus is therefore primarily on flame and melt ablation.

For the processes of melt and flame ablation, the expulsion of the melt is ensured by the force of an inert or active working gas. A coaxial and vertical flow of the for the laser beam cutting gas is common. This is unfavorable for ablation, as high pressure gradients result, whereas the velocity gradient is close to zero. This is optimized by shifting the stagnation point of the gas relative to the laser point of impact [6]. The biggest challenges for the flame ablation are the non-stationary process states. If too much energy is supplied and heat accumulates, the amount of heat supplied will exceed the amount of heat removed and the process proceeds unstable. Tönshoff et.al. describe this process state as "selfburning" [7]. Hoff et.al. provide an empirical model for a melt ablation process of 10 mm thick sheet steel [8]. They show that the production of a defined ablation groove with a depth of up to 7 mm at a volume ablation rate of over 1600 mm³/min is possible without exceeding a critical temperature of 300 °C. The horizontal nozzle offset, which depends on the possible ablation depth, turns out to be essential. In addition, it is shown that flame cutting (O_2) leads to uncontrolled exothermic reactions in the case of the investigated slim ablation grooves.

2. Process development

For the purpose of the defined steel plate weakening, results of laser flame and melt ablation tests are presented. Due to the maximum sheath thicknesses of the UXO, the influence of the laser, nozzle and motion parameters on the ablation depth and the temperature of the underside of the material are examined on the basis of 25 mm thick stainless steel sheets (S235).

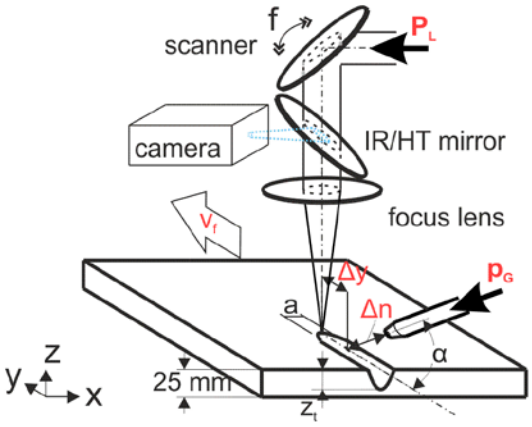

Fig. 2 Sketch of the process setup

2.1. Experimental setup and methods

For the investigations, the experimental set-up shown in Figure 2 was designed with an externally arranged gas supply. To create a wider ablation gap, a one-dimensional scanner was integrated into the optical path allowing a deflection of the laser beam with the frequency f by the amplitude a in x-direction (beam oscillation). A disk laser is used as the beam source with a beam quality of 8 mm*mrad. With the optics implemented, the laser beam has a focus diameter of 200 µm with a Rayleigh length of 1.3 mm. The beam is supplied perpendicular to the processing surface whereby the focus position is on the material surface. To ensure the mobility required for the application, the dimensions of the laser beam source must be as low as possible, resulting in the maximum laser power being limited to 2 kW. For process development, both the horizontal distance Δy of the nozzle to the laser axis in the range of 8 to 16 mm, and the coaxial distance Δn of the nozzle to the workpiece are varied. The nozzle angle α is determined by design to 45°. The process gas used is nitrogen 5.0 and oxygen 2.5 with a maximum pressure pG of 20 bar. According to the application, the speed movement vf is carried out by the movement of the head while the steel sheet remains fixed.

The evaluation of the process is based on the target values to be evaluated like the ablation depth zt and the temperature on the underside of the material. To record the depth of ablation by means of triangulation, a laser diode projects a line onto the material surface. This is recorded by a high-speed camera that is coaxially arranged and integrated into the processing head. In a second step, the pictures are analyzed by a software. Measurement accuracy based on defined notches has given a standard deviation of 0.25 mm for a measure number of 95. The temperature on the underside of the material is recorded using a thermal camera. For the evaluation of the measured value accuracy, comparative investigations were carried out with thermocouples. From 15 comparative measurements at different temperatures (80-250 °C), a standard deviation of 0.91 K was determined.

Based on the results of Hoff et.al. for the melt ablation (N_2) of 10 mm thick steel sheets, the following section 2.2 shows investigations for 25 mm thick sheets [8]. Additionally for the investigations with the scanner a process screening according to Shainin [9] was carried out.

2.2. Experimental results

The results of the process development for the melt ablation of 25 mm thick sheets are shown in Figure 3. The left diagram shows that the ablation depth increases with decreasing speed with importance depending on the nozzle offset Δy. This can be explained by the fact that the gas force of the nozzle, as shown in Scheme A, must attach to the lower end of the melt front, so that the pressure and thus the shear stress acts on the entire melt. If the impact point is too close to the laser axis (Scheme B), part of the melt is pushed back into the raised groove and fills it up. Furthermore, if the impact point is too far behind the beam axis, the resulting force is insufficient to push the entire melt out. Therefore, the optimal position is extremely dependent on the actual or maximum achievable ablation depth (scheme C), which in turn depends on the speed rate and the laser power. For the optimum nozzle distance, the ablation depth must be able to be estimated before the process. The temperature shown in the right diagram is only slightly influenced by the nozzle offset, since the introduced energy remains the same. The circles in the left diagram represent the depth variation of the ablation grooves over the length, in which the initial 10 mm of the groove area are excluded. As the radius of the circles increases, the variation decreases, so the quality of the groove gets worse. By optimizing the nozzle position, it can be seen in the diagram that the depth variation also decreases (circles become smaller). In addition, the depth variation tends to increase with decreasing speed. This shows that the maximum ablation depth is limited by the melt volume. As the ablation depth increases and the speed rates decrease, the expelled melt volume increases and is re-solidifying on the wall areas, which is associated with high depth variations over the ablation length. In addition the temperature rises on the underside of the material. The maximum achieved ablation depth z_t is 14.5 mm at parameters: P_L: 1.5 kW, p_G: 10 bar, v_f: 1 mm/s, Δy: 18 mm, Δn: 14.5 mm.

Studies on the approach of a successive increase in depth have shown that the ablation depths cannot be increased in a defined manner by means of linear multiple passages without groove enlargement. Due to the small groove width the expelled melt is pushed back into the groove produced by the first crossing and solidifies there.

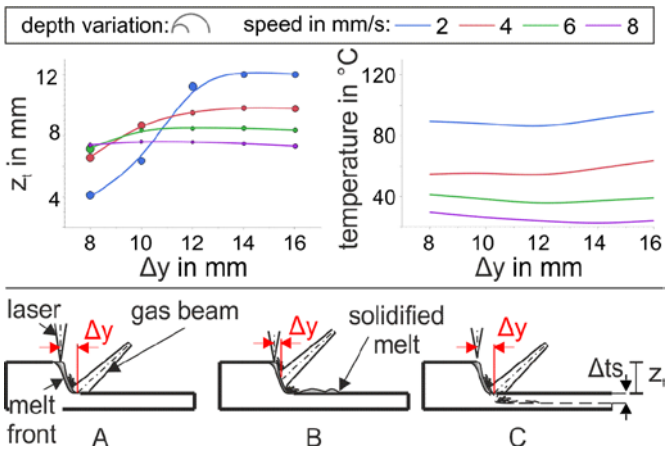

Fig. 3. Dependence of the ablation depth, depth variation and temperature of the nozzle offset. P_L 1.5 kW; Δn: 14mm.

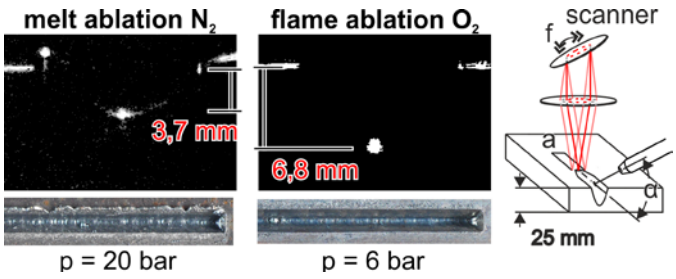

Fig. 4. Comparison of the scanner-supported flame and melt ablation. Parameter: P_l: 1.5 kW, v: 5 mm/s, F: 150 Hz, a: 4 mm

The following process strategy provides a widening of the ablation groove produced with the first pass, enabling a melt ejection for multiple passes. For this purpose, the laser beam oscillates with a defined amplitude and frequency in sinusoidal motion, perpendicular to the movement of the laser head. Figure 4 shows results of first basic ablation studies for this process strategy as the light section photographs and plan views of the removed grooves. The determined ablation depths illustrate that in a melt ablation process with the limited laser power of max. 2 kW, only very small ablation depths can be achieved; the energy per area is not enough to penetrate deeper into the material. Due to the additional exothermic energy supply by the melt ablation, significantly higher depths can be achieved. The selfburning effect, i.e. the uncontrolled burnup of the steel, is also a critical factor in this process strategy. However, this can be controlled by controlling the gas pressure.

Based on fundamental investigations for the determination of limit values, a process screening was carried out, from which the main influencing factors shown in red in Figure 2 laser power, speed, gas pressure, nozzle offset and nozzle distance emerged. These five process factors were used to perform the Central Composite Design (CCD) and allows statements to be made about the significance of the main effects, quadratic effects and two factor interactions of the investigated factors. With 36 trials, the number of trials required is many times lower than for a full factor plan (243 trials). On the basis of the results of this design of experiments, an empirical model could be determined by regression analysis (least square method). The influences on the ablation depth, whose probability that the observed effect or an even greater effect occurs only coincidentally is less than 5 % (Prob>|t|), are listed in Table 1.

Table 1. Effects for "Probability < |t|" < 5% for the ablation depth

Term	Estimate	Std Error	T Ratio	Prob> | t |
P_L	1.66 mm	0.12 mm	13.44	<0.0001
p_G	0.88 mm	0.12 mm	7.12	<0.0001
Δy	-0.33 mm	0.12 mm	-2.68	0.0132
v	-1.06 mm	0.12 mm	-8.59	<0.0001
Δn	-0.74 mm	0.12 mm	-6.02	<0.0001
P_L*p_G	0.34 mm	0.15 mm	2.24	0.0344
P_L*v	-0.34 mm	0.15 mm	-2.21	0.0368
p_G* p_G	-0.32 mm	0.10 mm	-3.11	0.0048
Δy* Δy	-0.24 mm	0.10 mm	-3.11	0.0283

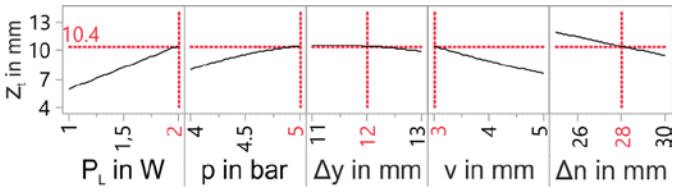

Fig. 5. Graphical forecast analysis for the laser flame ablation with pendulum motion. F: 150 Hz, a: 4 mm.

From the software calculations, the estimators of the terms, the associated standard errors and the t-value (Estimate / Std Error) are given. It can be seen that the significances for the main effects laser power, pressure, nozzle distance and speed are very high. In addition, there seems to be an interaction between the gas pressure and the speed with the laser power and a quadratic effect of the pressure und the nozzle offset. The red effects are in the upper 95 % confidence limit for the parameter estimate while the orange effects are in the upper 99 % confidence limit. The biggest influence is as assumed the laser power and the speed.

Figure 5 shows the model-derived forecast for the trend of the ablation depth for certain parameter settings. Predictions show an increasing ablation depth with increasing power and gas pressure and decreasing speed and nozzle offset. In the considered area, the nozzle offset has a comparatively small influence. As soon as operations take place outside of this range in reality, the ablation depth drops rapidly or the selfburning effect occurs. This can be explained by the above-described influence of the nozzle offset on the melt ejection. Due to the heat accumulation associated with a disadvantageous nozzle offset, higher temperatures lead to selfburning.

Verification experiments have shown that the model maps the process well in the considered parameter range. For the test results shown in figure 6, the model predicts an ablation depth of 10.4 mm. The well-reproducible ablation depth determined in the tests is 10 ± 0.4 mm. As shown, the created ablation gap is v-shaped and thereby very sharp. This is not optimal for the successive removal by a second passing. With an increased scanner amplitude of 10 mm, significantly wider u-shaped (i.e. wider on the ground) ablation forms could be achieved. Reproducible ablation depths of 8.5 ± 1 mm are possible with the process parameters P_L: 1.75 kW, v: 2 mm/s, Δy: 14 mm und p_G: 3 bar. The maximum temperatures on the underside of the material are 250 ± 20 °C. With averaged cross-sectional removal areas of 60 mm², this results in ablation rates of 7200 mm³/min. This achieved with the external gas supply ablation rate is much higher than previously known for flame ablation processes.

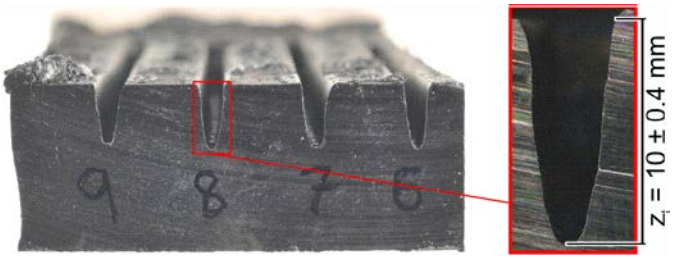

Fig. 6. Verification tests flame ablation with scanner. Parameter: P_L: 2 kW, p_N: 5 bar, v: 3 mm/s, Dy: 12 mm, Dn: 28 mm, a: 4 mm, F: 150 Hz.

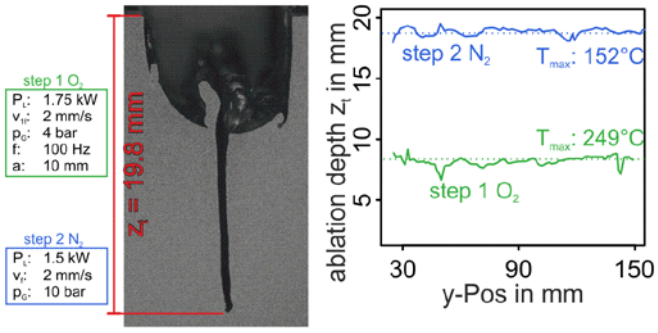

Fig. 7. Combination of a melt- and flame ablation test

Figure 7 shows results of a combined flame and melt ablation process. For the melt ablation process performed with the second pass, the laser focus is placed on the bottom of the groove created in the first pass. The wide groove produced in the flame ablation process with the scanner simplifies the melt ejection for the second pass. As illustrated in the cross section, maximum ablation depths of up to 20 mm can be achieved by means of this combined ablation strategy. The critical limit temperature of 300 °C is not exceeded. The right graph shows the trend of the ablation depth over the length of the ablation groove. As shown, in the process a very low depth variation of less than 1.5 mm is achieved. The y-Position starts at 30 mm, because at that point the settle area is over and the maximum ablation depth has been reached.

3. Conclusion

The results have shown that by means of an external gas supply and a combination of the melt- and flame ablation reproducible ablation grooves of up to 20 mm can be produced in the 25 mm thick sheets without exceeding critical temperature of 300 °C on the bottom. The achieved volume ablation rates of more than 7000 mm³/min are much higher than previously known. An empirical model could be set up and has been verified. In addition to the defuse on land, a huge proportion of UXO is under water. Therefore, the investigations will be extended to underwater processes in the future.

Acknowledgements

The project underlying this report was funded by the German Federal Ministry of Education and Research under founding reference 13N14155. The authors thank for the support.

Federal Ministry of Education and Research

References

[1] R. J. Rosen, “How many tons of world war ii munitions are found in germany each year?,” *The Atlantic*, Jan 3, 2014.
[2] E. U. S. E. P. Agency, “Technical fact sheet - 2,4,6 -trinitrotoluene (tnt),” January 2014.
[3] H. J. Fahrenwaldt, V. Schuler, and J. Twrdek, *Praxiswissen Schweißtechnik*. Springer Vieweg, 2014.
[4] F. Siegel, U. Klug, and R. Kling, “Extensive micro-structuring of metals using picosecond pulses – ablation behavior and industrial relevance,”

JLMN-Journal of Laser Micro/Nanoengineering, vol. 4, no. 2, pp. 104–110, 2009.

[5] D. Schubart, *Prozessmodellierung und Technologieentwicklung beim Abtragen mit CO2-Laserstrahlung*. Meisenbach Verlag Bamberg, 1998.

[6] W. C. Choi, *Analysis of the laser grooving process for ceramic materials*. Massachusetts Institute of Technology, 1989.

[7] H. Tönshoff and M. Stürmer, "Laserstrahlschneiden von crni-legierten feinblechen," *Metall (Berlin, West)*, vol. 44, no. 10, pp. 945–949, 1990. ger.

[8] C. Hoff, J. Hermsdorf, S. Kaierle, and L. Overmeyer, "Laser beam ablation of thick steel plates without affecting the material underneath," in *High-Power Laser Materials Processing: Applications, Diagnostics, and Systems VII*, 2018.

[9] W. Kleppmann, *Versuchsplanung: Produkte und Prozesse optimieren*. Carl Hanser Verlag GmbH & Company KG, 2016.